Chebyshev based spectral representations of neutron-star equations of state

Lee Lindblom[1] and Tianji Zhou[2]

[1]*Department of Physics, University of California at San Diego, San Diego, California 92093, USA*
[2]*Department of Physics and Astronomy, Haverford College, Haverford, Pennsylvania 19041, USA*

(Received 5 August 2024; accepted 16 September 2024; published 15 October 2024)

Causal parametric representations of neutron-star equations of state are constructed here using Chebyshev polynomial based spectral expansions. The accuracies of these representations are evaluated for a collection of model equations of state from a variety of nuclear-theory models and also a collection of equations of state with first- or second-order phase transitions of various sizes. These tests show that the Chebyshev based representations are convergent (even for equations of state with phase transitions) as the number of spectral basis functions is increased. This study finds that the Chebyshev based representations are generally more accurate than a previously studied power-law based spectral representation, and that pressure-based representations are generally more accurate than those based on enthalpy.

DOI: 10.1103/PhysRevD.110.083030

I. INTRODUCTION

Parametric representations of the neutron-star equation of state are used to model the poorly understood high-density material in the cores of these stars. The physical values of the parameters in these equation of state models can be determined by matching the macroscopic properties of the neutron-star models constructed from them (e.g. their masses, radii, or tidal deformabilities) with astronomical observations of those properties [1]. Fixing the equation of state parameters in this way provides a determination of the otherwise unobservable high-density neutron-star equation of state.

Faithful representations of the equation of state must satisfy basic thermodynamic stability and causality conditions along with minimal accuracy requirements. Thermodynamic stability requires the energy density of the material to increase monotonically as the pressure is increased. Causality requires the sound speed determined by the equation of state to be less than or equal to the speed of light. Equation of state representations must also be accurate enough to model any physical equation of state at a level commensurate with the accuracy of the available astrophysical observations. As the observations of neutron stars improve over time, useful representations should include a systematic way to match those improvements, e.g. by increasing the number of adjustable parameters. Suitable parametric representations should therefore be convergent in the sense that their accuracies increase as the as the number of parameters is increased.

A number of parametric representations of the neutron-star equation of state have been introduced in recent years [2–5]. All these representations appear to be sufficiently accurate to accommodate the precision of the currently available observations. Some of these representations ensure that the causality condition is satisfied. And some have been shown to be convergent in the sense that their accuracies can be increased by increasing the number of parameters. The most efficient representations, i.e. those providing the best accuracy for a given number of parameters, are based on spectral expansions [5].

The physical neutron-star equation of state may or may not have discontinuities caused by a phase transition. Constructing accurate parametric representations of equations of state with discontinuities is particularly challenging. The causal spectral representations that provide the most accurate representations (for a given number of parameters) of nuclear-theory based equations of state have recently been shown to be nonconvergent when used to represent equations of state with strong phase transitions [6]. The purpose of this paper is to determine whether Chebyshev polynomial based spectral expansions provide more robust and more accurate representations of neutron-star equations of state, including those with phase transitions.

Section II defines causal parametric representations of the neutron-star equation of state based on Chebyshev polynomial spectral expansions. These new representations include both pressure- and enthalpy-based versions of the equation of state. Section III describes the results of a series of numerical tests that measure the accuracy of these new representations, including comparisons with the previously studied spectral representations. The model equations of state used in these tests include a collection of nuclear-theory based neutron-star equations of state and a collection of model equations of state that include first- or second-order phase transitions. The implications of these results are discussed in Sec. IV.

II. CAUSAL CHEBYSHEV-BASED SPECTRAL REPRESENTATIONS

Shortly after their formation, the temperatures in the cores of neutron stars fall well-below the local Fermi temperature, so thermal contributions to the pressure and energy density become negligible [7]. The thermodynamic state of this high-density material should therefore be well-approximated by a barotropic equation of state: $\epsilon = \epsilon(p)$, where ϵ is the total mass-energy density and p is the pressure.

The speed of sound, v, in a barotropic fluid is determined by the equation of state: $v^2 = dp/d\epsilon$ [8]. These sound speeds are causal if and only if the velocity function Υ,

$$\Upsilon = \frac{c^2 - v^2}{v^2}, \tag{1}$$

is non-negative, $\Upsilon \geq 0$, where c is the speed of light.

A. Pressure-based spectral expansions

The velocity function Υ is determined by the equation of state: $\Upsilon(p) = c^2 d\epsilon/dp - 1$. Conversely, $\Upsilon(p)$ can be used as a generating function from which the standard equation of state, $\epsilon = \epsilon(p)$, can be determined by quadrature. The procedure for determining $\epsilon = \epsilon(p)$ from $\Upsilon(p)$ is summarized in Appendix A.

Causal parametric representations of the neutron-star equation of state can be constructed by expressing $\Upsilon(p, \upsilon_a)$ as a spectral expansion,

$$\Upsilon(p, \upsilon_a) = \exp\left\{\sum_{a=0}^{N_{\text{parms}}-1} \upsilon_a \Phi_a(p)\right\}, \tag{2}$$

where $\Phi_a(p)$ are the spectral basis functions and υ_a the spectral parameters. These expansions guarantee that $\Upsilon(p) \geq 0$ for every choice of υ_a. Therefore, any equation of state determined from one of these $\Upsilon(p, \upsilon_a)$ automatically satisfies the causality and thermodynamic stability conditions.

This study explores the use of Chebyshev polynomial basis functions in these spectral expansions,

$$\Upsilon(p, \upsilon_a) = \Upsilon_0 \exp\left\{\sum_{a=0}^{N_{\text{parms}}-1} \upsilon_a (1+y) T_a(y)\right\}, \tag{3}$$

where the $T_a(y)$ are Chebyshev polynomials. The variable y (defined below) is a function of the pressure having the property that $y = -1$ when $p = p_0$. The constants p_0 and Υ_0 are evaluated from the low-density equation of state at the point $p = p_0$ where it matches onto the high density spectral representation determined by Eq. (3). Choosing p_0 and Υ_0 in this way ensures that no artificial first- or second-order phase-transition discontinuity is introduced at the matching point.

Chebyshev polynomials are defined by the recursion relation $T_{a+1}(y) = 2yT_a(y) - T_{a-1}(y)$ with $T_0(y) = 1$ and $T_1(y) = y$. Spectral expansions using Chebyshev basis functions are well-behaved on the domain $-1 \leq y \leq 1$ [9]. Therefore, the variable y that appears in Eq. (3) has been defined as

$$y = -1 + 2\log\left(\frac{p}{p_0}\right)\left[\log\left(\frac{p_{\max}}{p_0}\right)\right]^{-1}, \tag{4}$$

to ensure that $-1 \leq y \leq 1$ for pressures in the range $p_0 \leq p \leq p_{\max}$. The factor $1 + y$ that appears in Eq. (3) ensures that $\Upsilon(p, \upsilon_a)$ has the limit, $\Upsilon(p_0, \upsilon_a) = \Upsilon_0$, for every choice of spectral parameters υ_a.

B. Enthalpy-based spectral expansions

For some purposes it is more convenient to use enthalpy-based representations of the neutron-star equation of state.[1] The enthalpy, $h(p)$, defined by

$$h(p) = \int_0^p \frac{dp'}{\epsilon(p')c^2 + p'}, \tag{5}$$

is a monotonically increasing function of the pressure p. Therefore the velocity function $\Upsilon(p)$ defined in Eq. (1) can also be expressed as a function of the enthalpy, $\Upsilon = \Upsilon(h)$.

Causal representations of the equation of state can also be generated using enthalpy-based spectral expansions of the velocity function $\Upsilon(h)$,

$$\Upsilon(h, \upsilon_a) = \exp\left\{\sum_{a=1}^{N_{\text{parms}}} \upsilon_a \Phi_a(h)\right\}, \tag{6}$$

where $\Phi_a(h)$ are a suitable set of enthalpy-based basis functions. Any equation of state constructed in this way automatically satisfies the causality and thermodynamic stability conditions; $\Upsilon(h, \upsilon_a) \geq 0$. The procedure for generating the enthalpy-based equation of state, $\epsilon = \epsilon(h, \upsilon_a)$ and $p = p(h, \upsilon_a)$, from $\Upsilon(h, \upsilon_a)$ is summarized in Appendix B.

This study explores the use of Chebyshev polynomials as spectral basis functions,

$$\Upsilon(h, \upsilon_a) = \Upsilon_0 \exp\left\{\sum_{a=0}^{N_{\text{parms}}-1} \upsilon_a (1+z) T_a(z)\right\}, \tag{7}$$

[1]The standard Oppenheimer-Volkoff [10] representation of the relativistic stellar structure equations has the property that $dp/dr \to 0$ at the surface of the star. This fact makes it difficult to accurately determine the location of the star's surface numerically. The enthalpy based representation of these equations [11] have the property that $dh/dr \to -M/[R(R-2M)]$, making it easier to compute the star's radius accurately in this case.

where the $T_a(z)$ are Chebyshev polynomials and the variable z is given by

$$z = -1 + 2\log\left(\frac{h}{h_0}\right)\left[\log\left(\frac{h_{\max}}{h_0}\right)\right]^{-1}. \tag{8}$$

The factor $1+z$ is included in Eq. (7) to ensure that $\Upsilon(h_0, \upsilon_k) = \Upsilon_0$ for every choice of υ_a.

This study compares the accuracies of the Chebyshev polynomial based spectral representations defined in Eq. (7) with those defined with the simple power-law spectral basis functions,

$$\Upsilon(h, \upsilon_a) = \Upsilon_0 \exp\left\{\sum_{a=1}^{N_{\text{parms}}} \upsilon_a \left[\log\left(\frac{h}{h_0}\right)\right]^a\right\}, \tag{9}$$

used in previous studies [4,5]. This study also compares the accuracy of the pressure-based Chebyshev representations defined in Eq. (3) with the enthalpy-based representations defined in Eq. (7).

III. NUMERICAL TESTS

This section describes a series of tests that measure the accuracy of the Chebyshev based spectral representations described in Sec. II. Best-fit spectral representations are constructed and their accuracies evaluated numerically for a variety of model neutron-star equations of state. Three different collections of reference equations of state are used in these tests. The first reference collection consists of 26 nuclear-theory based neutron-star equations of state[2] used by a number of studies to evaluate the accuracy of various parametric representations [2–5]. The second reference collection consists of equations of state with discontinuities representing first-order phase transitions having a range of sizes [6]. These equations of state were constructed by inserting a discontinuity into the GM1L nuclear-theory based equation of state.[3] The third reference collection is analogous to the second with discontinuities representing second-order phase transitions inserted with a range of sizes [6]. The reference equations of state used in these collections are represented as tables of enthalpy, pressure, and energy density values: $\{h_i, p_i, \epsilon_i\}$ for $1 \le i \le N_{\text{table}}$.

The numerical tests performed here construct spectral fits on the domain $p_0 = 1.20788 \times 10^{32}$ erg/cm$^3 \le p$. The upper limit of this domain, $p \le p_{\max}$, is taken to be the largest entry in the reference equation of state table. The constant Υ_0 is determined by differentiating the interpolation formula for the reference equation of state table.

A. Enthalpy-based tests

A primary motivation for this study was the finding in Ref. [6] that the enthalpy-based spectral representations using power-law basis functions were not convergent for equations of state with discontinuities caused by phase transition. Comparing the performance of the Chebyshev based representations introduced in Sec. II with the power-law based representations is therefore an important goal of this study.

Causal enthalpy-based spectral equation of state representations were computed following the methods described in Sec. II and Appendix B. The integrals used to construct the equation of state in Appendix B were performed numerically using Gaussian quadrature [15]. The resulting model equations of state are used to evaluate the energy densities, $\epsilon(h_i, \upsilon_a)$, at the tabulated enthalpy values, h_i, of the reference equations of state. These model energy-density values are then compared to the tabulated reference energy densities, ϵ_i, from the reference equation of state tables using the error measure,

$$\chi^2(\upsilon_a) = \frac{1}{N_{\text{table}}}\sum_{i=1}^{N_{\text{table}}}\left[\log\left(\frac{\epsilon(h_i, \upsilon_a)}{\epsilon_i}\right)\right]^2. \tag{10}$$

The optimal or "best-fit" parametric representations are found by minimizing $\chi^2(\upsilon_a)$ with respect to the spectral parameters υ_a.

The numerical calculations used in this study were performed using two independent codes to confirm the accuracy of the results. The minimizations of χ^2 were carried out numerically using a Fortran implementation of the Levenburg-Marquardt algorithm as described in Ref. [15], and using the scipy.optimize.least_squares implementation in Python [16]. The resulting minimum values of χ measure the accuracy of the best-fit parametric representations. These minimum values computed by the two codes agree to within a few percent for the new Chebyshev based representations.

Figure 1 illustrates the errors, χ, as a function of the number of spectral parameters, N_{parms}, for the best-fit models averaged over the reference collection of 26 nuclear-theory based neutron-star equations of state. The Chebyshev and power-law based representations have almost identical errors for $N_{\text{parms}} \le 5$ but the Chebyshev based models are more accurate than the power-law based models for larger N_{parms}. The Chebyshev based models show faster and cleaner exponential convergence than the

[2]The 26 nuclear-theory based equations of state used here are a causal subset of those used by Read *et al.* [2] in their study of the piecewise-polytropic representations of neutron-star equations of state. The abbreviated names of these equations of state are PAL6, SLy, APR1, WFF3, BBB2, BPAL12, MPA1, MS1, MS1b, PS, GS1, GS2, BGN1H1, GNH3, H1, H2, H3, H4, H5, H6, H7, PCL2, ALF2, ALF3. ALF4 and GM1L. See Ref. [2] for descriptions of these nuclear-theory models and the citations to the literature that define them.

[3]The GM1L equation of state was constructed in Ref. [12] from the GM1 equation of state [13] by adjusting the slope of the symmetry energy to agree with the established value, $L = 55$ MeV, using the formalism developed in Ref. [14].

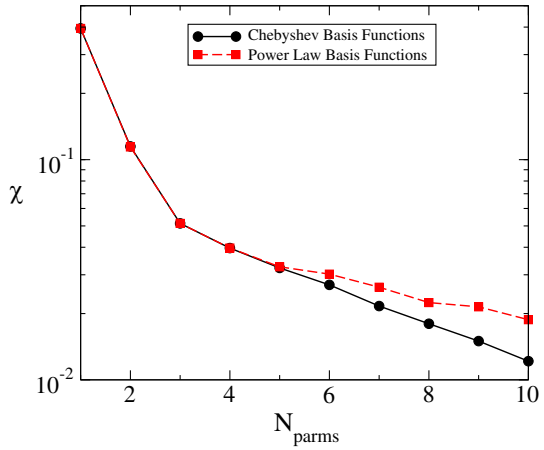

FIG. 1. Average modeling errors χ are illustrated as a function of N_{parms}, the number of spectral parameters, for the reference collection of 26 nuclear-theory based neutron-star equation of state models. The solid (black) curve gives results for the enthalpy-based Chebyshev basis functions, while the dashed (red) curve gives results for the simpler enthalpy-based power-law basis functions.

power-law bases models for these nuclear-theory based reference equations of state.

Figures 2 and 3 illustrate the best-fit modeling errors χ as functions of N_{parms} for the enthalpy-based Chebyshev polynomial spectral representations of the reference equations of state with first- or second-order phase transitions respectively. The individual curves in these figures represent equations of state with phase-transition discontinuities having sizes proportional to the parameter k. The $k = 0$ curves represent the GM1L equation of state with no discontinuity added, while the $k = 100$ curves correspond

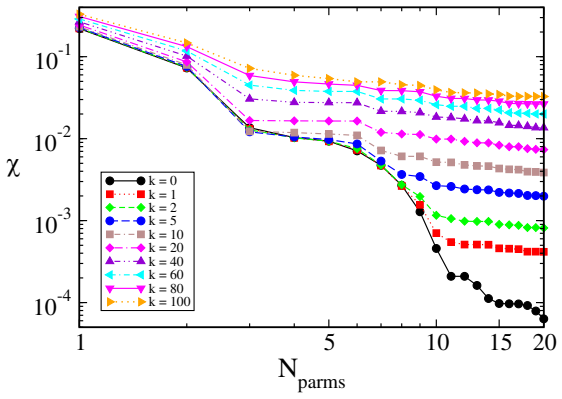

FIG. 2. Modeling errors χ for best-fit enthalpy-based Chebyshev spectral representations are illustrated as a function of N_{parms} for a collection of equations of state with first-order phase transitions. The k parameter is proportional to the size of the discontinuity caused by the phase transition, with $k = 0$ representing no discontinuity and $k = 100$ the maximum discontinuity allowed for stable neutron stars.

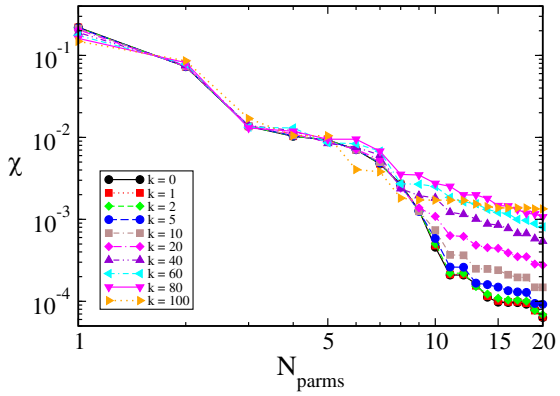

FIG. 3. Modeling errors χ for best-fit enthalpy-based Chebyshev spectral representations are illustrated as a function of N_{parms} for a collection of equations of state with second-order phase transitions of various sizes: $0 \le k \le 100$.

to the equations of state with the maximum physically allowed discontinuities, see Ref. [6] for details.

The linearity of the $\chi(N_{\text{parms}})$ curves for large N_{parms} in the log-log plots in Figs. 2 and 3 illustrate the convergence of the best-fit enthalpy-based Chebyshev spectral representations. The fitting errors for the equations of state with first-order phase transitions shown in Fig. 2 decrease with increasing N_{parms} as $\chi(N_{\text{parms}}) \propto N_{\text{parms}}^{-1/2}$ (approximately) for large N_{parms}, while the fitting errors for the equations of state with second-order phase transitions shown in Fig. 3 decrease as $\chi(N_{\text{parms}}) \propto N_{\text{parms}}^{-3/2}$ (approximately). The faster convergence of $\chi(N_{\text{parms}})$ by an additional power of N_{parms}^{-1} for the equations of state with the smoother second-order phase transitions is consistent with the expectations for algebraically convergent Chebyshev spectral expansions [9].

Enthalpy-based spectral representations using the simple power-law basis functions were studied in Ref. [6] for the reference equations of state with phase transition discontinuities. The graphs of $\chi(N_{\text{parms}})$ from that study did not show convergence for the equations of state with larger discontinuities. The detailed convergence graphs, analogous to Figs. 2 and 3, are given in Figs. 5 and 6 of Ref. [6], and will not be repeated here. The minimum χ values for the nonconvergent power-law based representations computed by the two codes used in this study agree qualitatively, but the differences in the error measures for the two codes are about an order of magnitude larger for the power-law based compared those for the Chebyshev based representations.

Figure 4 illustrates the relative accuracies of the enthalpy-based Chebyshev and the power-law spectral representations for averages over the reference collections of first- and second-order phase transitions. This figure illustrates the nonconvergence of the power-law representations for the larger values of N_{parms}. And these results show that the Chebyshev based spectral representations are

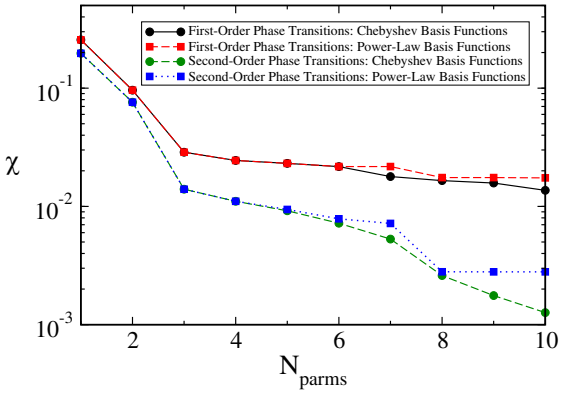

FIG. 4. Average modeling errors χ using enthalpy-based spectral expansions are illustrated as a function of $N_{\rm parms}$, the number of spectral parameters, for a collection of equations of state with first- and second-order phase transitions of various sizes, $0 \le k \le 100$.

somewhat more accurate than the power-law representations for larger values of $N_{\rm parms}$.

B. Pressure-based tests

Pressure-based spectral equations of state were computed following the method described in Sec. II and Appendix A. The resulting model equations of state are used to evaluate the energy densities, $\epsilon(p_i, \upsilon_a)$, at the tabulated pressure values, p_i, of the reference equations of state. These model energy-density values are then compared to the tabulated reference energy densities, ϵ_i, from the reference equation of state tables using the error measure,

$$\chi^2(\upsilon_a) = \frac{1}{N_{\rm table}} \sum_{i=1}^{N_{\rm table}} \left[\log\left(\frac{\epsilon(p_i, \upsilon_a)}{\epsilon_i} \right) \right]^2 . \qquad (11)$$

The best-fit representations are determined by minimizing $\chi(\upsilon_a)$ over the spectral parameters υ_a. The resulting best-fit error measures $\chi(N_{\rm parms})$ for the pressure-based Chebyshev representations are compared in this section to the best-fit results for the enthalpy-based Chebyshev representations.

Figure 5 illustrates the average errors, χ, as a function of the number of spectral parameters, $N_{\rm parms}$, obtained for the best-fit models of the reference collection of 26 nuclear-theory based neutron-star equations of state. The (black) solid curve represents the results using the enthalpy-based Chebyshev spectral representations, while the (red) dotted curve represents the results using the pressure-based Chebyshev spectral representations. These results show that the pressure-based representations have average errors roughly half those of the enthalpy-based representations for each value of $N_{\rm parms}$ in this collection of nuclear-theory based equations of state.

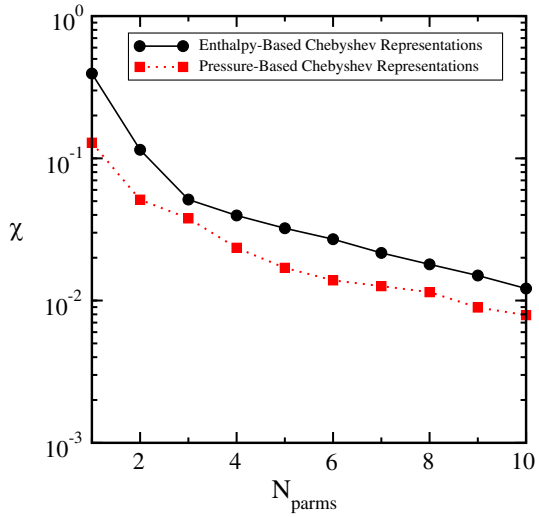

FIG. 5. Average modeling errors χ using pressure-based Chebyshev representations compared to those using enthalpy-based Chebyshev representations of 26 nuclear-theory based equation of state models.

The pressure-based spectral expansions using Chebyshev basis functions are convergent. The detailed plots of $\chi(N_{\rm parms})$ for the reference collections of equations of state with first- or second-order phase transitions are qualitatively similar to Figs. 2 and 3 so they will not be included here. Figure 6 illustrates the average values of $\chi(N_{\rm parms})$ for the collections of equations of state with first- or second-order phase transitions. As was the case for the enthalpy-based representations, the fitting errors for the equations of state with first-order phase transitions decrease

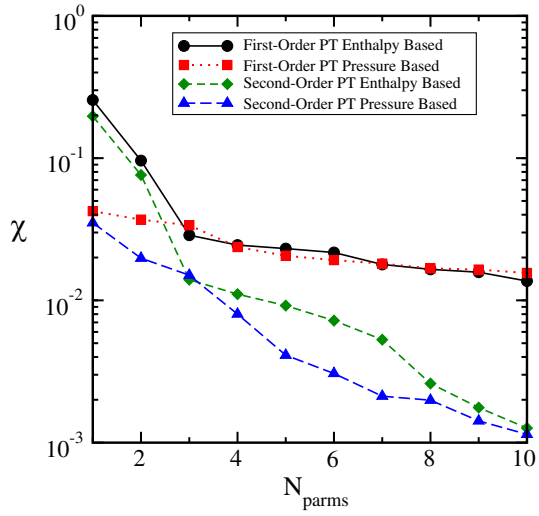

FIG. 6. Average modeling errors χ using pressure-based Chebyshev spectral representations compared to those using enthalpy-based Chebyshev spectral representations. Comparisons are given for the averages over the collections of reference equations of state with first- or second-order phase transitions of various sizes.

with increasing $N_{\rm parms}$ as $\chi(N_{\rm parms}) \propto N_{\rm parms}^{-1/2}$ (approximately), while the fitting errors for the equations of state with second-order phase transitions decrease as $\chi(N_{\rm parms}) \propto N_{\rm parms}^{-3/2}$ (approximately). Figure 6 shows that the pressure-based Chebyshev representations are significantly better than the enthalpy-based representations for $N_{\rm parms} < 3$. For larger values of $N_{\rm parms}$ the pressure-based representations have more or less the same accuracy as the enthalpy-based representations of the equations of state with first-order phase transitions. The pressure-based representations are uniformly better than the enthalpy-based representations with $N_{\rm parms} > 3$ for equations of state with second-order phase transitions.

IV. DISCUSSION

This study focused on two questions. Are the enthalpy-based spectral expansions using Chebyshev polynomial basis functions an improvement over the nonconvergent previously studied expansions using power-law basis functions? How does the accuracy of the pressure-based Chebyshev representations compare to the accuracy of the enthalpy-based Chebyshev representations?

The tests summarized in Sec. III A show that the enthalpy-based spectral representations using Chebyshev polynomial basis functions are generally more accurate those using power-law basis functions. The Chebyshev based representations are shown to be convergent where the power-law based representations were not. When applied to equations of state with discontinuities caused by phase transitions, the convergence rates of the Chebyshev based representations become algebraic at rates appropriate for spectral representations.

The tests summarized in Sec. III B show that the pressure-based spectral representations using Chebyshev polynomial basis functions are (almost) uniformly better than the analogous enthalpy-based representations. These pressure-based representations are convergent with the same convergence rates as the enthalpy-based representations. However the pressure-based representations have average modeling errors that are roughly half those of the enthalpy-based representations for the reference collection of 26 nuclear-theory based neutron-star equations of state. The pressure-based representations with $N_{\rm parms} < 3$ are also significantly more accurate than the enthalpy-based representations for the equations of state with first- or second-order phase transitions.

ACKNOWLEDGMENTS

We thank Fridolin Weber for providing us with the GM1L equation of state table used in this study, including the literature citations to its provenance. This research was supported in part by the National Science Foundation Grants No. 2012857 and No. 2407545 to the University of California at San Diego, USA. T. Z. was supported by a Haverford College KINSC Summer Scholars fellowship.

APPENDIX A: CAUSAL PRESSURE-BASED REPRESENTATIONS

This appendix summarizes the procedure developed in Ref. [4] for using the velocity function $\Upsilon(p)$ defined in Eq. (1) as a generating function that determines the pressure-based equation of state; $\epsilon = \epsilon(p)$.

The definition of the velocity function $\Upsilon(p)$ can be rewritten as the ordinary differential equation,

$$\frac{d\epsilon(p)}{dp} = \frac{1}{c^2} + \frac{\Upsilon(p)}{c^2}. \tag{A1}$$

This equation can be integrated to determine the pressure-based equation of state, $\epsilon = \epsilon(p)$:

$$\epsilon(p) = \epsilon_0 + \frac{p - p_0}{c^2} + \frac{1}{c^2}\int_{p_0}^{p} \Upsilon(p')dp'. \tag{A2}$$

Causal spectral representations of the equation of state can then be constructed using Eq. (A2) with the pressure-based representations of $\Upsilon(p, \upsilon_a)$ given in Sec. II.

APPENDIX B: CAUSAL ENTHALPY-BASED REPRESENTATIONS

This appendix summarizes the procedure developed in Ref. [4] for using the velocity function $\Upsilon(h)$ defined in Eq. (1) as a generating function that determines the enthalpy-based equation of state: $\epsilon = \epsilon(h)$ and $p = p(h)$. Enthalpy based representations of the equation of state are more useful than the standard pressure-based representations for some purposes. For example these representations make it easier to solve the more accurate and more efficient enthalpy-based representations of the Oppenheimer-Volkoff neutron-star structure equations [11].

The definition of the enthalpy, h, in Eq. (5) implies an expression for $dp/dh = \epsilon c^2 + p$. Similarly, the definition of the velocity function, Eq. (1), provides an expression for $d\epsilon/dh$:

$$\Upsilon(h) = c^2\frac{d\epsilon}{dp} - 1 = c^2\frac{d\epsilon}{dh}[\epsilon(h)c^2 + p(h)]^{-1} - 1. \tag{B1}$$

Together these definitions provide a system of first-order ordinary differential equations for $\epsilon(h)$ and $p(h)$,

$$\frac{dp}{dh} = \epsilon c^2 + p, \tag{B2}$$

$$\frac{d\epsilon}{dh} = \left(\epsilon + \frac{p}{c^2}\right)[\Upsilon(h) + 1]. \tag{B3}$$

These equations can be reduced to quadratures,

$$p(h) = p_0 + (\epsilon_0 c^2 + p_0) \int_{h_0}^{h} \mu(h') dh', \tag{B4}$$

$$\epsilon(h) = -\frac{p(h)}{c^2} + \left(\epsilon_0 + \frac{p_0}{c^2}\right)\mu(h), \tag{B5}$$

where $p_0 = p(h_0)$ and $\epsilon_0 = \epsilon(h_0)$ represent a point on the equation of state curve, and $\mu(h)$ is given by

$$\mu(h) = \exp\left\{\int_{h_0}^{h} [2 + \Upsilon(h')] dh'\right\}. \tag{B6}$$

Equations (B4)–(B6) determine a causal spectral representation of the equation of state for any of the enthalpy-based spectral expansions $\Upsilon(h, \upsilon_a)$ defined in Sec. II.

[1] L. Lindblom, AIP Conf. Proc. **1577**, 153 (2014).
[2] J. S. Read, B. D. Lackey, B. J. Owen, and J. L. Friedman, Phys. Rev. D **79**, 124032 (2009).
[3] L. Lindblom, Phys. Rev. D **82**, 103011 (2010).
[4] L. Lindblom, Phys. Rev. D **97**, 123019 (2018).
[5] L. Lindblom, Phys. Rev. D **105**, 063031 (2022).
[6] L. Lindblom, Phys. Rev. D **110**, 043018 (2024).
[7] A. Y. Potekhin, J. A. Pons, and D. Page, Space Sci. Rev. **191**, 239 (2015).
[8] L. D. Landau and E. M. Lifshitz, *Fluid Mechanics* (Pergamon Press, New York, 1959).
[9] J. P. Boyd, *Chebyshev and Fourier Spectral Methods*, 2nd ed. (Dover Publications, New York, 1999).
[10] J. R. Oppenheimer and G. M. Volkoff, Phys. Rev. **55**, 374 (1939).
[11] L. Lindblom, Astrophys. J. **398**, 569 (1992).
[12] W. M. Spinella, Ph.D. thesis, Claremont Graduate University & San Diego State University, 2017.
[13] N. K. Glendenning and S. A. Moszkowski, Phys. Rev. Lett. **67**, 2414 (1991).
[14] S. Typel, G. Röpke, T. Klähn, D. Blaschke, and H. H. Wolter, Phys. Rev. C **81**, 015803 (2010).
[15] W. H. Press, S. A. Teukolsky, W. T. Vetterling, and B. P. Flannery, *Numerical Recipes in FORTRAN*, 2nd ed. (Cambridge University Press, Cambridge, England, 1992).
[16] P. Virtanen, R. Gommers, T. E. Oliphant, M. Haberland, T. Reddy, D. Cournapeau, E. Burovski, P. Peterson, W. Weckesser, J. Bright *et al.*, Nat. Methods **17**, 261 (2020).